Neural reprogramming in retinal degenerations

Robert E. Marc[1], **Bryan W. Jones**[1], **James R. Anderson**[1], **Krista Kinard**[1], **David W. Marshak**[2], **John H. Wilson**[3], **Theodore Wensel**[3], and **Robert J. Lucas**[4]

1 *Department of Ophthalmology, John A. Moran Eye Center, University of Utah*

2 *Department of Neurobiology & Anatomy, University of Texas Medical School at Houston*

3 *Department of Biochemistry & Molecular Biology, Baylor College of Medicine*

4 *Faculty of Life Sciences, University of Manchester*

Abstract

Purpose—Early visual defects in degenerative diseases such as retinitis pigmentosa (RP) may arise from phased remodeling of the neural retina. We sought to explore the functional expression of ionotropic (iGluR) and group III, type 6 metabotropic (mGluR6) glutamate receptors in late-stage photoreceptor degenerations.

Methods—Excitation mapping with organic cations and computational molecular phenotyping were used to determine whether retinal neurons displayed functional glutamate receptor signaling in rodent models of retinal degenerations and a sample of human RP.

Results—After photoreceptor loss in rodent models of RP, bipolar cells lose mGluR6 and iGluR glutamate-activated currents, while amacrine and ganglion cells retain iGluR-mediated responsivity. Paradoxically, amacrine and ganglion cells show spontaneous iGluR signals *in vivo* even though bipolar cells lack glutamate-coupled depolarization mechanisms. Cone survival can rescue iGluR expression by OFF bipolar cells. In a case of human RP with cone sparing, iGluR signaling appeared intact, but the numbers of bipolar cells expressing functional iGluRs was double that of normal retina.

Conclusions—RP triggers permanent loss of bipolar cell glutamate receptor expression, though spontaneous iGluR-mediated signaling by amacrine and ganglion cells implies that such truncated bipolar cells still release glutamate in response to some non-glutamatergic depolarization. Focal cone-sparing can preserve iGluR display by nearby bipolar cells, which may facilitate late-RP photoreceptor transplant attempts. An instance of human RP provides evidence that rod bipolar cell dendrite switching likely triggers new gene expression patterns and may impair cone pathway function.

Introduction

Many early visual defects in degenerative diseases such as retinitis pigmentosa (RP) may arise from phased tissue remodeling and functional reprogramming of the neural retina. Most retinal degenerations are progressive diseases that begin with a period (*phase 1*) of photoreceptor or retinal pigmented epithelium cell stress and subsequent phenotype deconstruction. In *phase 2* the outer nuclear layer is remodeled via photoreceptor death, bystander killing, phagocytotic ablation, and entombment of the remnant retina beneath a seal of Müller cell processes. *Phase*

Corresponding Author: Robert E. Marc, Department of Ophthalmology, John A. Moran Eye Center, 65 Medical Dr, University of Utah, Salt Lake City, UT 84132, 801.585.6500 laboratory/office, 801.541.4573, cell, 801.587.7845 fax, robert.marc@hsc.utah.edu.

3 is characterized by slow, persistent revisions of the neural retina via neuronal death, cell migration and *de novo* neurite and synapse formation.[1,2]

Most analyses of retinal degenerations have focused on events surrounding phase 2 and photoreceptor death. But abnormal reprogramming occurs in all phases and can begin prior to photoreceptor death[1]. During early phase 2, ganglion cell light responses change in many ways, culminating in loss of ON responses and paradoxical preservation of OFF responses[3] (also see Stasheff, S.F. *Invest. Ophthalmol. Vis. Sci.* 2006 47: E-Abstract 5771). Even after complete photoreceptor loss, waves of robust ganglion cell spiking occur in the *Pde6b*[rd1] mouse retina (Stasheff, S.F. *Invest. Ophthalmol. Vis. Sci.* 2004; 45, E-Abstract 5070), mimicking focal scintillation illusions common in human RP.[4] These and other studies suggest that widespread alterations in connectivity and signaling emerge in the neural retina after photoreceptor loss. However, most electrophysiological methods are limited to sampling few (often unidentified) cells in retinas lacking photoreceptors and have not been able to provide strong insights regarding the cellular participants, scope and nature of neural reprogramming in retinal degenerations. Similarly, most classical immunocytochemistry has given only a qualitative view of structural disassembly and potential activity patterns in degenerating retinas.

We have attempted a more complete description of reprogramming by using excitation mapping[5,6] to image neuronal signaling histories across disease states with single-cell resolution and comprehensive coverage.[7] We explored the ability of retinal neurons to signal via glutamate receptor mechanisms *in vivo* and with *in vitro* ligand activation in wild type mice and *rdcl* and *hrhoG* mutant mice expressing rapid photoreceptor degenerations. In addition, we were able to perform *in vitro* excitation mapping in a sample of human RP retina. These experiments reveal reprogramming events in bipolar cells that may impact all forms of proposed retinal rescue strategies.

METHODS

Animals

Control *wt* C57BL/6J mice were obtained from The Jackson Laboratories. Rodless-coneless *rdcl* (*rd/rd cl*) mice (from the Lucas laboratory) are homozygous for *Pde6b*[rd1] and carry a transgene driving a diphtheria toxin-based lesion of cone photoreceptors[8]. Congenic C3H/He mice were the corresponding controls for the *rdcl* mice. The *hrhoG* mice (from the Wensel and Wilson laboratories) were GFP-tagged human rhodopsin knock-in models[9] that undergo rapid rod degeneration and generate significant bystander killing of cones. All of these mutants generally represent comprehensive RP models, although *hrhoG* mice harbor small islands of cone sparing similar to *Pde6b*[rd1] mice[10]. Eyes from adult male and female olive baboons (*Papio anubis*) were obtained at necropsy from the Southwest Foundation for Biomedical Research (San Antonio, TX). All methods for anesthesia and euthanasia conform to institutional animal care and use authorizations at the authors' respective institutions and the ARVO Statement for the Use of Animals in Ophthalmic and Visual Research.

Human specimen

A left eye posterior pole from a male RP patient with impaired night vision and functional central vision was obtained from the Lion's Eye Bank donor pool at the University of Utah within two hours postmortem. The Lion's Eye Bank donor procurement and distribution complies with the Declaration of Helsinki. All data were de-identified in accord with the HIPAA Privacy Rule.

AGB mapping in vivo

Neuronal signaling was tracked *in vivo* by intravitreal injections of 1-amino-4-guanidobutane (AGB), an organic cation that preferentially permeates activated iGluR channels of the α-amino-3hydroxyl-5-methylisoxazole-4-propionic acid (AMPA), kainate (KA) and N-methyl-D-aspartate (NMDA) classes[5] as well as channels gated by the ON bipolar cell mGluR6 receptor.[11,12] Control C3H/He pnd 60–90 mice (n=4) and congenic *rdcl* mice (n=4) received deep urethane anesthesia via intraperitoneal injection and intravitreal injections of ≈ 0.5–1 μL 25 mM AGB (agmatine sulfate, A-7127, Sigma Aldrich, St Louis, MO) in physiological saline. Two of each group were dark adapted and the others maintained for a further 45 minutes of anesthesia under constant fluorescent room lighting (≈ 3.0 10^4 photons/second/μm^2 integrated over 400–700 nm) prior to euthanasia with pentobarbitol. After brief Halothane® induction pnd 495 *hrhoG* mice (n=10) received deep urethane anesthesia via intraperitoneal injection (1g/Kg). The anterior pole of the eye was slit at the limbus with a scalpel tip and the vitreous flooded with 5 μl Ames medium supplemented with 25 mM AGB. The animals were maintained for 45 minutes under constant fluorescent room lighting (≈ 2–2.9 10^4 photons/second/μm^2 integrated over 400–700 nm) prior to sacrifice. There were no detectable differences in labeling in dark or light adapted mutant mice. There were adaptation differences in normal mice but these are beyond the scope of this report.

AGB mapping *in vitro*

Twelve eyes from pnd 240–495 *hrhoG* mice (n=12) and seven eyes from C57Bl6J adult mice (n=4) were used for *in vitro* mapping. Eyes were enucleated from euthanized mice, the cornea cut away and the lens gently removed. On occasion, the lens adhered to the retina in *hrhoG* mice and these samples were discarded without further processing. Twelve eyecups were successfully processed. Baboon eyes (n=2) were maintained in carboxygenated Ames medium (Sigma Aldrich, St Louis, MO) for ≈ 2 hours prior to incubation, precisely matching the postmortem delay in the human RP samples. Human and baboon posterior poles were segmented by razor into large on-choroid pieces and as isolated retinal samples mounted on filters[15] and incubated. All samples were immersed in carboxygenated Ames medium + 5 mM AGB at 35°C and activated with various glutamate receptor agonists[5–7] for 10 min, followed by quenching in fixative. For all comparisons presented here, retinas were activated with 25 μl KA (Sigma Aldrich, St Louis, MO). We have previously established that KA + AGB selectively and comprehensively visualizes populations of neurons expressing the pharmacological phenotype of AMPA/KA receptors.[6]

Sample Processing

Tissues were fixed overnight in buffered 2.5% glutaraldehyde, 1% formaldehyde and resin embedded as previously described.[12] Single or stacked samples were serially sectioned at 250 nm onto 12-spot Teflon®-coated slides (Cel-Line; Erie Scientific Inc), probed with IgGs targeting various molecules, and visualized with silver-intensified 1.4 nm gold granules conjugated to goat anti-rabbit or goat anti-mouse IgG (Nanoprobes, Yaphank, NY).[12] Small molecule IgGs (anti-L-aspartate, anti-L-glutamate, anti-glycine, anti-glutathione, anti-L-glutamine, anti-taurine, anti-GABA and anti-AGB) were provided by Signature Immunologics Inc (Salt Lake City, UT). Anti-LWS1 (i.e. red and green) cone opsin was obtained from Chemicon International Inc (Temecula, CA) and anti-rhodopsin rho1D-4 was a kind gift from Robert Molday.

Imaging

All images of immunoreactivity were captured as mosaicked tiles of eight-bit 1388 pixel × 1036 line frames under voltage regulated tungsten halogen flux with a variation of 1.2 ± 0.6%/min (mean ± sd). Images were captured with a Peltier-cooled QImaging Fast 1394 QICAM

(QImaging, Burnaby, BC, Canada) and autotiled with a Syncroscan montaging system (Synoptics Inc, Frederick, MD) and a Scan 100×100 stage (Märzhäuser Wetzlar GMBH & Co, Germany). Images were analyzed without filtering or scaling. [7,13] Serial images were aligned with algorithms from PCI Remote Sensing, Inc. (Richmond Hill, Ontario, Canada).

Analysis and Display

Individual cell classes or superclasses were extracted from monochrome images by K-means clustering[6,12,13] using pixel-based (PCI Remote Sensing, Inc., Richmond Hill, Ontario, Canada) and object-based algorithms (CMPView V1.0, University of Utah, © J.R. Anderson) built in MATLAB 7.2 (The MathWorks, Natick Massachusetts). Cluster classes were visualized as theme maps and univariate pixel probability density histograms[7] of AGB signals in each cell class were extracted with CellKit V2.4OSX (University of Utah, © R. Marc) built in the IDL programming language (ITT Visual Information Solutions, Boulder, CO). Each histogram represents all of the possible 8-bit pixel values associated with a class and is proportional to log concentration.[7,12] Each histogram was smoothed with a 5 bin Lee filter. Small differences in background signal between preparations were shifted by assigning the minimum signal of Müller cells (an unresponsive cohort) to zero. Profiles of absolute AGB signals were measured across the inner plexiform layer, from level 0 (the amacrine cell layer - inner plexiform layer border) to level 100 (the ganglion cell layer - inner plexiform layer border). Signaling at each level was determined as the mean PV across a 1 pixel thick × 300 pixel wide strip (0.28 μm × 85 μm) for each inner plexiform layer level and boxcar filtered to achieve 1 μm resolution in the scan path. GABA and glycine signals in the same region were binarized, logically ANDed with AGB signals to form images of pure GABAergic and glycinergic neurite responses and profiled over the same path by computing the nonzero signal means. No normalization was used. Adobe® PhotoShop® CS2 9.01 was used for final image generation. Display images were generated by linear contrast stretch of each channel using min-max pixel values of 30 and 220 respectively.

The quantitative power of excitation mapping of identified cells has been discussed[7,12] but sampling issues are emphasized here. AGB signaling in a sample of OFF BCs is a reliable measure of the signaling mechanisms over the entire population. For example, in over 50 teleost fish, 250 rabbit, 50 mouse and 3 normal primate samples, 25 μM KA has *never* failed to elicit robust AGB responses from ≈ 1/3 of the BC population. The probability of any single sample showing few or no activated cells after a run of 350 successes is $<10^{-100}$, assuming a worst-case random binomial outcome probability. Even a single negative response outcome from a dystrophic retina is highly significant.

Terminology

As in previous publications[11–13] we use the standard single-letter biochemical code for each amino acid (G glycine, E glutamate) augmented by notations for non-protein amino acids and other small molecules (B AGB, τ taurine, γ GABA). Color images are true-color *rgb*-mapped images where each molecule is mapped to a channel. For example γ.B.E → *rgb* implies that GABA signals are mapped to the red channel, AGB signals to the green channel and glutamate signals to the blue channel. This convention is used throughout the text and on the figures.

Results

Signaling in degenerating retinas during remodeling was mapped in rodent models and human RP. Both *rdcl* and *hrhoG* mice rapidly display photoreceptor degeneration and enter phase 3 remodeling in less than 100 days. A large cohort of aged *hrhoG* was analyzed as well. A sample of human RP retina with cone sparing allowed *in vitro* documentation of functional iGluR display after nearly complete loss of rods and extensive extrafoveal cone transformation.

Endogenous and activated glutamatergic signaling

We tested *in vivo* signaling in *rdcl* mice during early phase 3 (pnd 60–90). Endogenous neuronal signaling in the wild type (*wt*) mouse retina, probed over a 45-minute period in mesopic light demonstrated that all retinal bipolar cells were extremely active via iGluR or mGluR6 mediated signaling (Fig. 1a,b). Variations in amacrine cell and ganglion cell signaling arise from differences in AMPA and NMDA receptor expressions across cell classes[6,7]. The *rdcl* model displays a markedly different pattern (Fig. 1c,d), which is quantitatively compared across neuronal classes by signal butterfly histograms (Fig. 1e). Virtually all *rdcl* bipolar cells were silent even though the amacrine and ganglion cell targets of bipolar cells manifest glutamatergic drive. Bipolar cell-like profiles sometimes showed AGB content, but these were rare (<1% of identified bipolar cells). Some *rdcl* neurons are even more active than *wt* neurons, shown by the upward shift in the ganglion and amacrine cell histograms (Fig. 1e). This is consistent with Stasheff's (see above) evidence of enhanced spontaneous activity in ganglion cells of the *Pde6b*[rd1] mouse after loss of all light responses. Since all known glutamatergic inputs to ganglion cells arise from cone bipolar cell synapses in the intact retina, this finding argues for spontaneous glutamate release from cone bipolar cells in the *rdcl* retina. However, *rdcl* amacrine cell response histograms are strongly bimodal and the weaker mode is likely partly derived from glycinergic and GABAergic amacrine cells arborizing in the rod bipolar cell terminal layer. Profile plots (Fig. 1F) show that the *in vivo* activities of glycinergic and GABAergic amacrine cell neurites faithfully track the total inner plexiform layer AGB signal at every level. While activity is robust in layers driven by cone bipolar cells in all mice, signals are negligible in the proximal zone driven by rod bipolar cells in *rdcl* mice and are indistinguishable from Müller cell labeling (see Fig. 1D). This suggests that rod bipolar cells are relatively hyperpolarized in early phase 3.

Does bipolar cell signaling ever recover? To explore this we tested ten pnd 300–450 *hrhoG* mice and found no endogenous bipolar cell signaling, but widespread, albeit weak amacrine cell and ganglion cell signaling (Figure 2). Once bipolar cells lose the ability to express functional glutamate receptors, they apparently do not reactivate expression even after extensive phase 3 remodeling.

Though *rdcl* and *hrhoG* OFF bipolar cells failed to display channel permeation *in vivo*, their iGluR-gated channels should be closed in the absence of photoreceptor drive. To explore whether they are persistently inactivated in retinal degenerations we used iGluR agonists to drive AGB permeation into OFF bipolar cells.[5,6] Activation of *wt* retinas leads to AGB permeation into ≈ ⅓ of bipolar cells (Figure 3A,B) with varied patterns of amacrine and ganglion cell activation, as expected. However, application of KA to late phase 3 hrhoG retinas from twelve separate animals (Fig. 3C,D,F) revealed iGluR-mediated permeation events in amacrine and ganglion cells but absent from bipolar cells. Regardless of the genetic nature of the degeneration, downstream phenotype reprogramming apparently results in persistent loss of functional iGluR expression. There are apparent changes in iGluR expression in other neurons as well, as the ability of KA to activate amacrine cell and ganglion cells is significantly poorer than in control retinas (Fig. 3F). The inability of dystrophic retinas to generate any responses characteristic of OFF bipolar cells is highly significant and the chance of even a single instance of failure to activate bipolar cells with KA is $<10^{-100}$ (see **METHODS**).

Partial bipolar cell rescue by cones

Focal cone survival may attenuate these fates. Remodeling is delayed in slow degenerations (e.g. *Prph2*[Rd2] and *pcd* mice) where altered cones survive long after rod loss.[2] Even the *Pde6b*[rd1] mouse exhibits sparing of small clusters of cone-like cells.[10] Similarly, the *hrhoG* model displays small cone clusters surrounded by retina lacking photoreceptors. These cones expressed no detectable LWS1 opsins (not shown), but the proximal neural retina remained

well-organized and harbors bipolar cells with strong KA-driven AGB signals (Fig. 4A,B). Thus, in one individual, bipolar cells in cone-free regions lose iGluR signaling ability while those near remodeled cones preserve iGluR expression. While we have not reconstructed these zones, our impression is that bipolar cells further than 50 μm from remnant cones cannot be activated, implying that direct contact is necessary.

It is difficult to quantitate the scope of bipolar cell preservation near tiny cone clusters, but we were able to acquire a human RP retina for *in vitro* excitation mapping and comparison with normal primate retina (Fig. 5 A,B). The RP retina had regionally lost 90–100% of rods but possessed numerous remodeled cones, most of which lacked outer segments. Over 90% of the cones displayed no detectable LWS1 opsin (Fig. 5 C,D). However, iGluR-mediated drive of all neuronal classes was robust in the RP retina and included many bipolar cells, as demonstrated by KA activation in vertical sections (Fig. 5A,B) and horizontal section theme maps (Fig. 5 E,F). The theme maps were derived from datasets containing up to 32,000 inner nuclear layer neurons in a single field. We used object-based clustering (see **METHODS**) to classify iGluR-driven OFF (green), and iGluR-insensitive cone ON (red) and rod ON (blue) bipolar cells based on characteristic signatures[6]. Though the signaling pattern in the human RP retina generally resembled normal primate retina, the fraction of responsive bipolar cells was anomalously high. In normal primate retina, the proportions (OFF cone:ON cone:ON rod) of the bipolar cell classes were ≈ 40:30:30, whereas in the RP retina it was ≈ 75:20:05 (Fig. 5d–g). The probability of a single normal mammalian sample showing this result is 2.7×10^{-6} based on a normal distribution derived from the mean OFF bipolar cell fractions of 3 primate, 5 rabbit, and 3 mouse samples of KA-activated AGB permeation. Paradoxically, there was no evidence of bipolar cell loss in the RP retina. These findings suggest that rod bipolar cells activated expression of iGluRs.

Discussion

Retinal degenerations lead to reprogramming of the neural retina in at least three ways. The canonical mGluR6 and iGluR pathways that define ON and OFF bipolar cell disappear. The ability of the neural retina to self-signal is unmasked. Cone-sparing degenerations admit partial rescue of rod bipolar cells, but evokes anomalous iGluR expression.

Impaired bipolar cell function in retinal degenerations

The absence of AGB permeation in bipolar cells of the *rdcl* and *hrhoG* mouse models is consistent with findings in the *Pde6b*[rd1] mouse that bipolar cells retract their dendrites upon loss of rods and cones[15–17] and glutamate fails to elicit responses in isolated bipolar cells.[18] AGB mapping *in vivo* reveals no cation current at all in most cells, implying deconstruction of the mGluR6 mechanism. Similarly, most OFF bipolar cells lack any evidence of functional iGluR expression. Though Strettoi et al.[15–17] showed mislocalization of mGluR6 immunoreactivity to the axons of some remnant bipolar cells, our data suggest that it is not functional, similar to rhodopsin mislocalization. The persistent loss of iGluR and mGluR6 components suggests that bipolar cells undergo a more complex process of phenotype deconstruction than just a simple loss of dendrites. Even *Xenopus* oocytes reliably display functional iGluRs produced by injected ectopic mRNA and oocytes have no dendrites. Survivor bipolar cells in late phases of retinal degenerations seem to have lost either the ability to express any glutamate receptor genes or properly traffic any glutamate receptor proteins.

Self-signaling in the retina

One paradoxical outcome of *in vivo* excitation mapping is the discovery that both amacrine and ganglion cells are extremely active through iGluR-mediated channels, though bipolar cells are not. What is the source of this activation? Bipolar cells form the only known glutamatergic

synapses in the inner plexiform layer. If so, they clearly release sufficient glutamate to activate amacrine and ganglion cells *in vivo*. Glutamate release requires depolarization, but that cannot arise from mGluR6 or iGluR channel-mediated cation currents. Photoreceptor loss may unmask endogenous oscillations in amacrine cell membrane potential and calcium levels[19] which, via GABA or glycine release, may modulate the voltage of bipolar cell presynaptic terminals, triggering glutamate release onto amacrine and ganglion cell targets. Any alternate hypothesis would require a widespread, effective but *undiscovered* glutamatergic cell type. Regardless of the provenance of self-signaling, it appears to weaken over time. It is intriguing that both the strength of self-signaling and the clinical incidence of photopsias diminish with time.

Bipolar cell rescue and reprogramming in cone-sparing RP

RP occurs as cone-sparing and cone-decimating versions. In the cone-decimating *Pde6b*[rd1] and the *hrhoG* mouse models, patches of altered cones persist, though they are embedded in a Müller cell seal. Carter-Dawson et al.[14] showed that such cones in the *Pde6b*[rd1] mouse retain synaptic ribbons and classical contacts. Our finding that bipolar cells retain functional iGluR signaling subjacent to patches of opsin-deficient cones implies that synaptic contact accesses signaling mechanisms sufficient to preserve dendritic function in bipolar cells, though we do not know what those mechanisms are. Though this may not seem surprising, there is abundant evidence rod phototransduction defects also impair rod:neuron communications and lead to retraction of rod bipolar cell dendrites prior to rod death.[15–17] While we know that total loss of photoreceptors leads to loss of functional glutamate receptor display in both ON and OFF bipolar cells, the fate of rod bipolar cells in cone-sparing disease is less clear.

In both cone-sparing transgenic pig RP P347S rhodopsin model[20] and cone-decimating rodent P23H models[21], rod bipolar cells are able to abandon dying rods and respectively adopt persistent or transient ectopic non-ribbon contacts with survivor cones (Fig. 6A). Further, analyses of the rodless *nrl* mouse clearly demonstrate that rod bipolar cells are quite capable of forming functional synapses with cones during development.[22] The key questions are whether target switching by mature neurons in RP leads to functional or fictive synapses and functional or corruptive signaling.

The acquisition of a human RP retina for *in vitro* excitation mapping was fortuitous as it allowed a unique, robust test of bipolar cell fates. In addition to massive rod loss, survivor cones were structurally anomalous and most lacked LWS1 opsin expression. Consistent with results in mouse, even these extremely altered cones preserved robust bipolar cell iGluR expression. But the fraction of OFF-like responses nearly doubled and rod bipolar cell signatures effectively disappeared, even though we could detect no bipolar cell loss. The only plausible explanations we have for this phenomenon are that rod bipolar cells survived by switching contacts to cones and responded via iGluRs.

Based upon models of glutamate diffusion from mammalian cone synapses,[23] ectopic contacts likely do not access adequate glutamate levels for mGluR6 transduction activation (Fig. 6B). We argue that survivor rod bipolar cells assume the phenotype of OFF cone bipolar cells to recover signaling capacity. Paradoxical focal KA receptor immunore-activity has previously been associated with ON bipolar cells[24,25], suggesting constitutive low level transcription of iGluR message, though iGluR-coupled currents are normally undetectable in ON bipolar cells. [26] On balance, ectopic contacts appear functional.

What are the circuitry consequences? If some cones remain photosensitive, phenotype reprogramming will transform the dominant mammalian scotopic pathway[27] (Fig. 6C) into a collision circuit (Fig. 6D) ill-suited for cone vision. The conservative conclusion is that rescue of rod bipolar cells by survivor cones forms corruptive circuits.

Implications

The degenerating retina is dynamic and manifests alterations resembling hippo-campal reprogramming in epilepsy, where loss of afferent control, changes in connectivity and changes in iGluR expression mediate aberrant signaling.[28] Reprogramming impacts every strategy for ameliorating RP by constraining intervention windows for genetic or molecular therapy; by potentially generating non-visual signaling network instabilities that may impair the efficacies of prosthetic implants; and by preventing or corrupting therapeutic progenitor cell engraftment. For example, the finding that a small fraction of time-selected fetal rod progenitor cells can develop into a mature-like rod phenotype and contact survivor bipolar cells in some rodent degeneration models is very promising.[29] As the engraftments were made in genetic models characterized by extended cone survival, and/or *prior* to phase 2 seal consolidation, the ability of such cells to engraft or properly drive reprogrammed phase 3 retinas of the profoundly blind remains a critical question.

References

1. Marc RE, Jones BW, Watt CB, Strettoi E. Neural Remodeling in Retinal Degeneration. Prog Ret Eye Res 2003;22:607–655.

2. Jones BW, et al. Retinal remodeling triggered by photoreceptor degenerations. J Comp Neurol 2003;464:1–16. [PubMed: 12866125]

3. Pu M, Xu L, Zhang H. Visual response properties of retinal ganglion cells in the Royal College of Surgeons dystrophic rat. Invest Ophth Vis Sci 2006;47:3579–3585.

4. Delbeke J, et al. Electrical stimulation of anterior visual pathways in retinitis pigmentosa. Invest Ophthalmol Vis Sci 2001;42:291–297. [PubMed: 11133881]

5. Marc RE. Mapping glutamatergic drive in the vertebrate retina with a channel-permeant organic cation. J Comp Neurol 1999;407:47–64. [PubMed: 10213187]

6. Marc RE. Kainate activation of horizontal, bipolar, amacrine, and ganglion cells in the rabbit retina. J Comp Neurol 1999;407:65–76. [PubMed: 10213188]

7. Marc RE, Jones BW. Molecular phenotyping of retinal ganglion cells. J Neurosci 2002;22:412–427.

8. Lucas RJ, Freedman MS, Munoz M, Garcia-Fernandez JM, Foster RG. Regulation of the mammalian pineal by non-rod, non-cone, ocular photoreceptors. Science 1999;284:505–507. [PubMed: 10205062]

9. Chan F, Bradley A, Wensel TG, Wilson JH. Knock-in human rhodopsin-GFP fusions as mouse models for human disease and targets for gene therapy. Proc Natl Acad Sci 2004;101:9109–9114. [PubMed: 15184660]

10. Carter-Dawson LD, LaVail MM, Sidman RL. Differential effect of the rd mutation on rods and cones in the mouse retina. Invest Ophthalmol Vis Sci 1978;17:489–98. [PubMed: 659071]

11. Kalloniatis M, Sun D, Foster L, Haverkamp S, Wässle H. Localization of NMDA receptor subunits and mapping NMDA drive within the mammalian retina. Visual Neurosci 2004;21:587–597.

12. Marc RE, Kalloniatis M, Jones BW. Excitation mapping with the organic cation AGB^{2+} Vision Res 2005;45:3454–3468. [PubMed: 16139860]

13. Marc RE, Murry RF, Basinger SF. Pattern recognition of amino acid signatures in retinal neurons. J Neurosci 1995;15:5106–29. [PubMed: 7623139]

14. Marc RE, Cameron DA. A molecular phenotype atlas of the zebrafish retina. J Neurocytol 2001;30:593–654. [PubMed: 12118163]

15. Strettoi E, Pignatelli V. Modifications of retinal neurons in a mouse model of retinitis pigmentosa. Proc Natl Acad Sci 2000;97:11020–11025. [PubMed: 10995468]

16. Strettoi E, Porciatti V, Falsini B, Pignatelli V, Rossi C. Morphological and functional abnormalities in the inner retina of the rd/rd mouse. J Neurosci 2002;22:5492–5504. [PubMed: 12097501]

17. Strettoi E, Pignatelli V, Rossi C, Porciatti V, Falsini B. Remodeling of second-order neurons in the retina of rd/rd mutant mice. Vision Res 2003;43:867–877. [PubMed: 12668056]

18. Varela C, Igartua I, De la Rosa EJ, De la Villa P. Functional modifications in rod BCs in a mouse model of retinitis pigmentosa. Vision Res 2003;43:879–885. [PubMed: 12668057]

19. Firth SI, Feller MB. Dissociated GABAergic retinal interneurons exhibit spontaneous increases in intracellular calcium concentration. Visual Neurosci 2006;23:807–814.

20. Peng Y-W, Hao Y, Petters RM, Wong F. Ectopic synaptogenesis in the mammalian retina caused by rod photoreceptor-specific mutations. Nature Neurosci 2000;3:1121–1127. [PubMed: 11036269]

21. Cuenca N, et al. Regressive and reactive changes in the connectivity patterns of rod and cone pathways of P23H transgenic rat retina. Neuroscience 2004;127:301–317. [PubMed: 15262321]

22. Strettoi E, Mears AJ, Swaroop A. Recruitment of the rod pathway by cones in the absence of rods. J Neurosci 2004;24:7576–7582. [PubMed: 15329405]

23. Devries S, Li W, Saszik S. Parallel processing in two transmitter microenvironments at the cone photoreceptor synapse. Neuron 2006;50:735–748. [PubMed: 16731512]

24. Haverkamp S, Grünert U, Wässle H. Localization of kainate receptors at the cone pedicles of the primate retina. J Comp Neurol 2001;436:471– 486. [PubMed: 11447590]

25. Calkins DJ. Localization of ionotropic glutamate receptors to invaginating dendrites at the cone synapse in primate retina. Visual Neurosci 2005;22:469–477.

26. Euler T, Schneider H, Wässle H. Glutamate responses of bipolar cells in a slice preparation of the rat retina. J Neurosci 1996;16:2934–44. [PubMed: 8622124]

27. Deans MR, Volgyi B, Goodenough DA, Bloomfield SA, Paul DL. Connexin36 is essential for transmission of rod-mediated visual signals in the mammalian retina. Neuron 2002;36:703–712. [PubMed: 12441058]

28. Epsztein J, Represa A, Jorquera I, Ben-Ari Y, Crepel V. Recurrent mossy fibers establish aberrant kainate receptor operated synapses on granule cells from epileptic rats. J Neurosci 2005;25:8229–8239. [PubMed: 16148230]

29. MacLaren RE, et al. Retinal repair by transplantation of photoreceptor precursors. Nature 2006;444:203–207. [PubMed: 17093405]
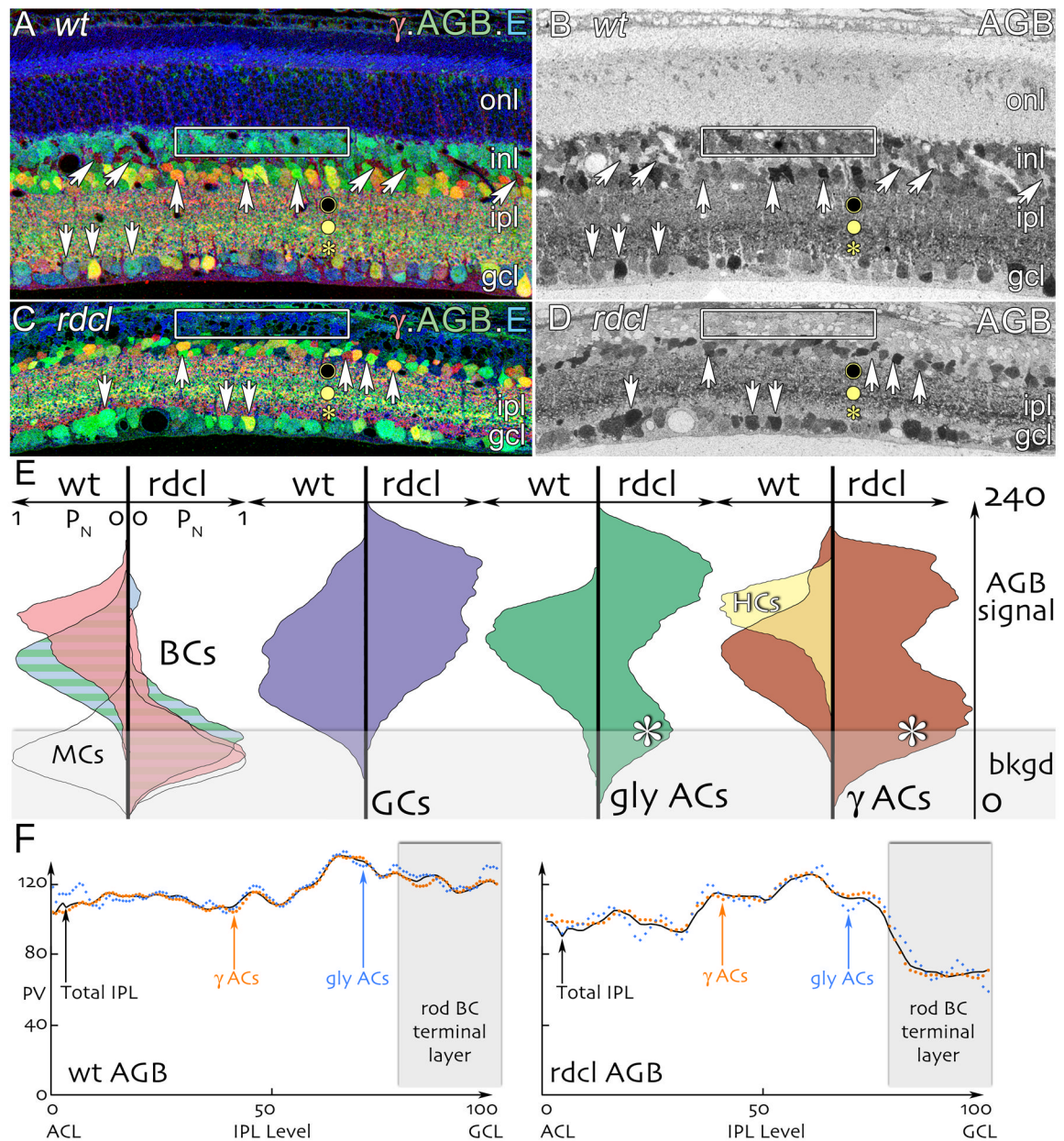
Figure 1.
Endogenous glutamatergic signaling in *wt* and mutant mouse retinas under mesopic light conditions tracked by AGB permeation. High resolution images of boxed regions are available at http://prometheus.med.utah.edu/~marclab/mss/IOVS.html). **A,B** Endogenous signaling in *wt* mouse retinas. (**A**) γ.B.E → *rgb* (GABA.AGB.glutamate) mapped and (**B**) greyscale AGB images show that nearly all neurons are active and display AGB permeation. The box in the inner nuclear layer (inl) contains AGB-rich cells, indicating that all bipolar cell classes are responsive. Different strengths of amacrine cell (upward arrows) and ganglion cell (downward arrows) responses are consistent with normal retinal activity patterns. Signaling in the inner plexiform layer (ipl) is relatively uniform with strong bands in the cone OFF (black dot), cone ON (yellow dot) and rod ON (yellow aster) layers. **C,D** Endogenous signaling in *rdcl* mouse retinas. (**C**) γ.B.E → *rgb* mapped and (**D**) greyscale AGB images demonstrate that only

amacrine and ganglion cells are endogenously active. The inl box contains only unlabeled neurons, indicating no AGB permeation. Different strengths of amacrine cell (upward arrows) and ganglion cell (downward arrows) responses imply variation in endogenous activity. Signaling in the ipl is strong in the cone OFF and ON layers, but very weak in the rod ON layer. All images are 0.3 mm wide; onl, outer nuclear layer; ipl, inner plexiform layer; gcl, ganglion cell layer. **E**, Univariate AGB butterfly histograms comparing endogenous wt and rdcl retinal activity for specific cell classes: BCs bipolar cells, GCs ganglion cells, gly ACs glycinergic amacrine cells and γ ACs GABAergic amacrine cells. The ordinate on each of the plots represents AGB signal strength as an 8-bit grey pixel value. The abscissas for each plot are normalized probability densities (P_N), allowing direct comparison of *wt* (left wing) and mutant (right wing) cell class response patterns. Each histogram represents over 100–500 adjacent cells, except for horizontal and ganglion cell histograms, representing 50–100 adjacent cells. BC Histogram (left): the wt Müller cell signal profile (M, white histogram) defines the background (bkgd) level, shaded across all histograms. Endogenous AGB permeation signals of *wt* bipolar cells are segmented by cluster analysis[13] into ON cone BCs (pale red) and all other BCs (blue-green striped) and are significantly above background. All *rdcl* bipolar cells are below background, implying little or no endogenous signaling. GC Histogram: both *wt* and *rdcl* GC signals are broadly dispersed with stronger compression to high responses in *wt* animals. Gly AC Histogram: *wt* glycinergic amacrine cells yield a broad pseudo-unimodal response, while *rdcl* ACs generate a clearly bimodal response with a large fraction of nearly unresponsive cells, many of which project to the rod-driven layer of the inner plexiform layer *. γ AC Histogram (right): *wt* GABAergic amacrine cells also yield a broad pseudo-unimodal response, while *rdcl* amacrine cells generate a bimodal response, similar to glycinergic amacrine cells and with similar rod dependencies *. All horizontal cells (HCs) are uniformly highly responsive in *wt* retinas, but none were identified in the *rdcl* retina. **F**, Profiles of *in vivo* signaling in the inner plexiform layer of *wt* (left) and *rdcl* (right) mice. Absolute AGB PV signals at each level of the inner plexiform layer were plotted for total inner plexiform layer neurites (black trace), GABAergic neurites (orange dotted trace) and glycinergic neurites (blue diamond trace) as described in **Methods**. The rod bipolar cell terminal layer is indicated by the shaded box.
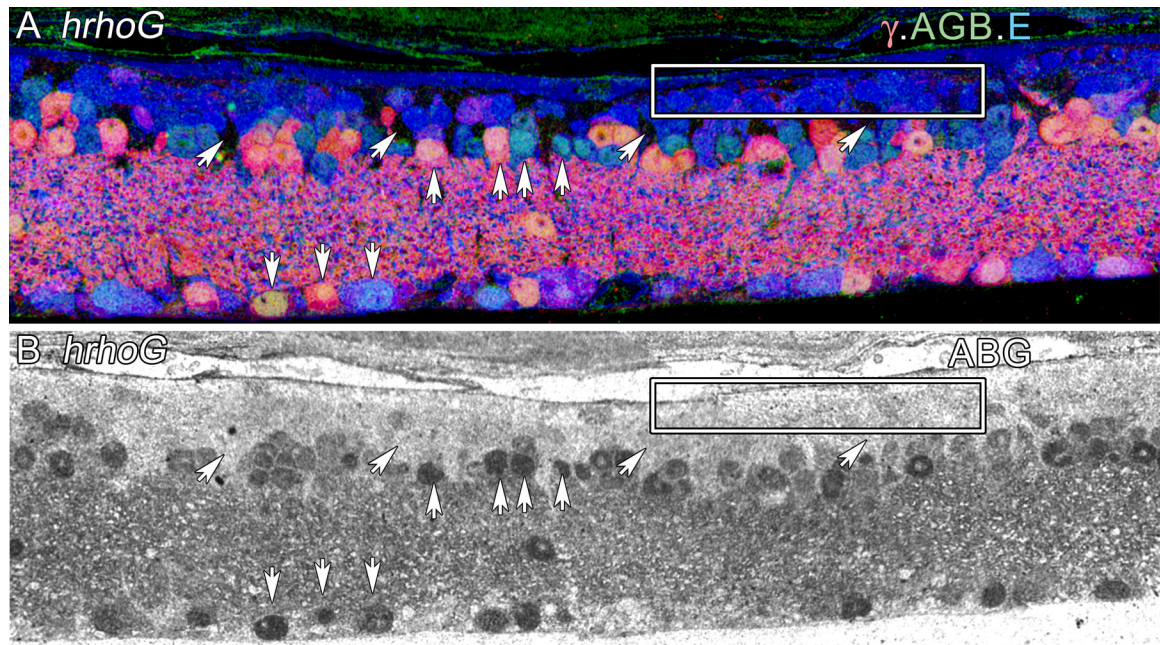
Figure 2.
Endogenous signaling phase 3 *hrhoG* mutant mouse retinas tracked by AGB permeation. Symbols have the same meanings as in Figure 1. (**A**) γ.B.E → rgb (GABA.AGB.glutamate) mapped and (**B**) greyscale AGB images images demonstrate that only amacrine and ganglion cells are endogenously active. The inner nuclear layer box contains only lightly labeled neurons, indicating no AGB permeation. Different, albeit modest amacrine (upward arrows) and ganglion cell (downward arrows) responses are consistent with intrinsic signaling. Signaling in the inner plexiform layer (ipl) is relatively uniform but diffuse, indicating remodeling of rod signaling layers. All images are 0.3 mm wide; onl, outer nuclear layer; ipl, inner plexiform layer; gcl, ganglion cell layer.
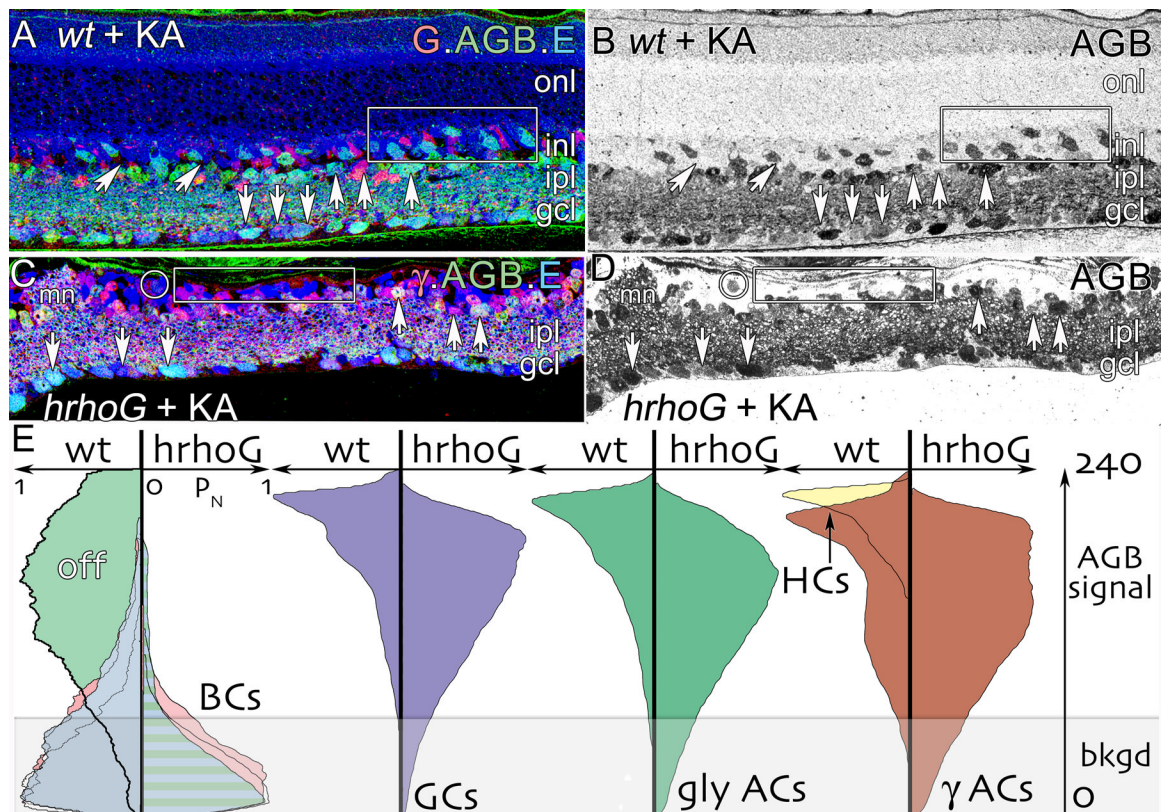
Figure 3.

A,B KA-driven (25 μM) signaling in *wt* mouse retinas. Symbols have the same meanings as in Figure 1. (**A**) G.B.E (glycine.AGB.glutamate) → *rgb* mapped and (**B**) greyscale AGB images show that many, but not all neurons are responsive. The inl box contains a mixture of responsive and unresponsive bipolar cells, suggesting selective visualization of the normal iGluR-driven OFF bipolar cell cohort. Most amacrine (upward arrows) and ganglion cells (downward arrows) have strong responses, whereas Müller cells are unresponsive (angled arrows). Signaling in the ipl is uniformly strong, consistent with the pervasive expression of AMPA receptors in all layers. **C,D** KA-driven (25 μM) signaling in *hrhoG* mouse retinas. (**C**) G.B.E → *rgb* mapped and (**D**) greyscale AGB images show that only amacrine and ganglion cells are responsive. The inl box contains only unresponsive bipolar cells. The circle contains a single weakly responsive cell. Amacrine and ganglion cell responses are weaker and more variable than *wt*. All images are 0.3 mm wide. **E**, Univariate AGB signal histograms comparing KA-activated *wt* and *hrhoG* retinal activity for specific cell classes. **BC histogram** (left): KA-activated AGB permeation signals of wt bipolar cells are segmented into responsive OFF (pale green) and non-responsive ON bipolar cells (pale blue and red striped). Nearly all *hrhoG* bipolar cells are below background, implying little or no iGluR-mediated signaling. **Gly AC, γ AC and GC histograms**: both *wt* and *hrhoG* amacrine and ganglion cell signals demonstrate broad response profiles, with most cells exhibiting vigorous responses in the *wt* animals and a broad dispersion in the mutants. Horizontal cells were identified only in *wt* retinas.
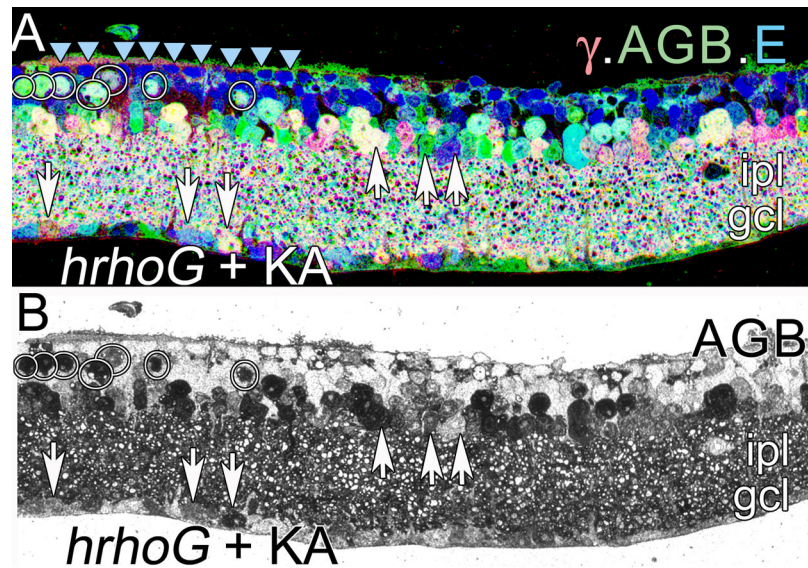
Figure 4.
A,B KA-driven (25 μM) signaling in *hrhoG* mouse retinas in focal regions of cone survival. Patches of transformed cones are indicated by the blue triangles. (**A**) γ.B.E → *rgb* mapped and (**B**) greyscale AGB images show that KA-responsive bipolar cells are common near cones, demonstrating local persistence of iGluR expression. Amacrine and ganglion cell signals are also robust. All images are 0.3 mm wide.
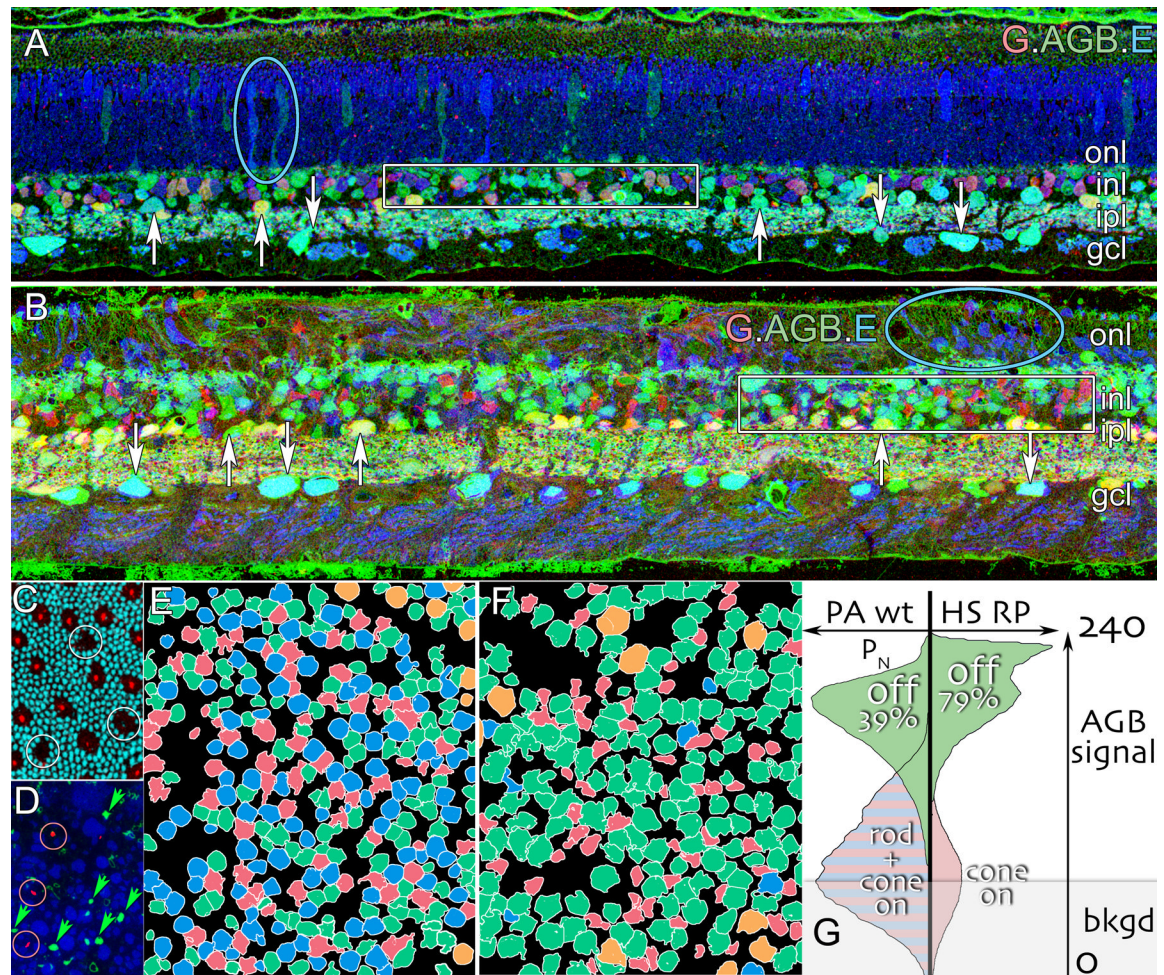
Figure 5.
KA-driven (25 μM) signaling in (**A**) normal baboon and (**B**) human RP retina. Symbols have the same meanings as in Figure 1. (**A**) G.B.E (glycine.AGB.glutamate) → *rgb* mapped and (**B**) greyscale AGB images show that that many, but not all neurons are responsive. The onl ellipses illustrate (**A**) normal and (**B**) aberrant cone morphologies in the blue glutamate channel. The inl boxes contain mixtures of responsive and unresponsive bipolar cells, allowing selective visualization of the normal iGluR-driven OFF bipolar cell cohort for each condition. Most amacrine (upward arrows) and ganglion cells (downward arrows) have strong responses. Signaling in the ipl is uniformly strong, consistent with the pervasive expression of AMPA receptors in all layers. **C,D** Rhodopsin and LWS1 (red and green) cone opsin immunoreactivity in normal and dystrophic primate retinas. **C** Rhodopsin is expressed uniformly in rods (cyan) while most cones express LWS1 opsin immunoreactivity. Circled areas represent putative blue cones. **D** Remnant rhodopsin-containing (green, arrows) or LWS1 cone opsin-containing (red, circles) outer segments are rare and short. Most cones (blue) are highly modified and lack any detectable opsin immunoreactivity. **E,F** KA-driven (25 μM) signaling in normal and dystrophic primate retinas segmented by cluster analysis[16] into ON rod (blue), ON cone (red) and active OFF cone bipolar cell (green) cohorts; horizontal cells are orange and Müller cells or unclassified cells are black. Image widths: **A,B** 0.6 mm; **C,D** 47 μm; **E** 120 μm; **F** 77 μm. **G**, Scaled univariate butterfly histograms of KA-activated bipolar cell signals for normal baboon (*Papio anubis*) and dystrophic human retinas. Left wing (PA wt): OFF bipolar cells (pale green) comprise 39% and non-responsive ON cone and rod bipolar cells (pale blue and red striped)

comprise 71% of all BCs in normal perhiperal primate retina. Right wing (HS RP, *H. sapiens* RP): OFF bipolar cells (pale green) comprise 79% and non-responsive ON cone bipolar cells (pale red) comprise 21% of all bipolar cells in the dystrophic retina. Rod bipolar cells comprise less than 3% of the remnant cells
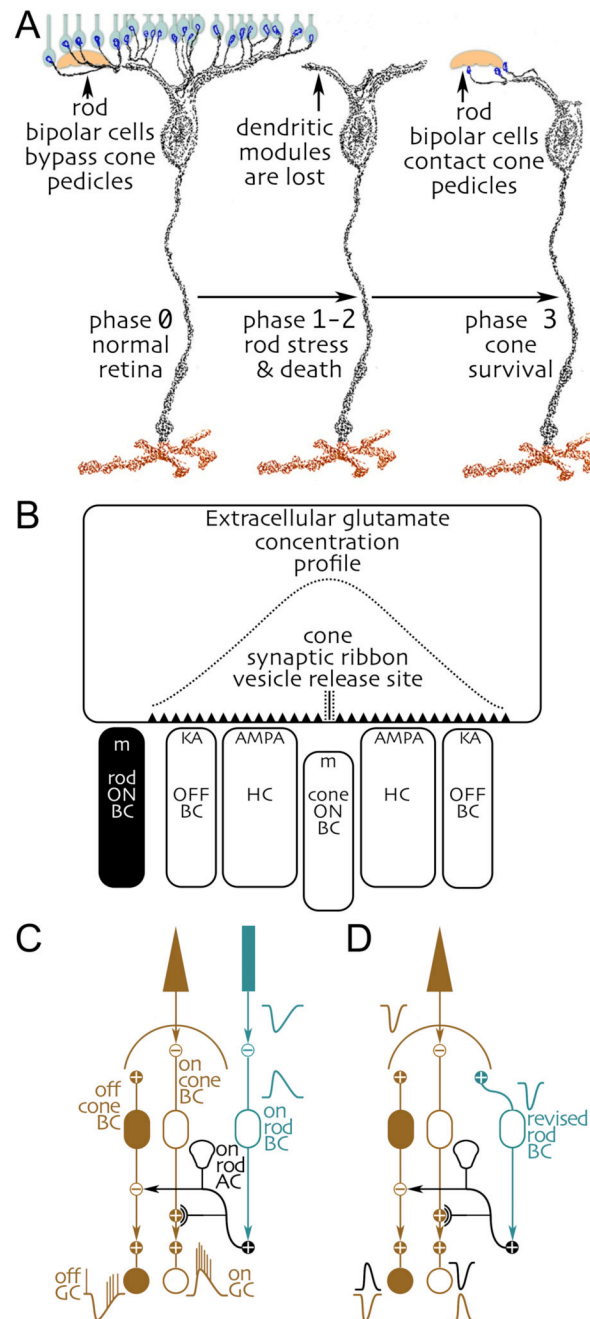
Figure 6.
Signaling and bipolar cell reprogramming. **A** Rod bipolar cell remodeling in cone-sparing RP. Normal "phase 0" rod bipolar cells bypass cone synapses to contact rods. In phase 1–2 RP, rod stress and death trigger dendrite retraction and in persistent phase 2 cone survival, some rod bipolar cells successfully make ectopic contacts with cones. **B** The cone synaptic ribbon zone viewed as a flattened 2D structure with central glutamate release from a ribbon site, laterally displaced dendrites of target cells, and a gradient of extracellular glutamate. Ectopic dendrites from rod ON bipolar cells (black) likely access too little glutamate to activate the mGluR6 (m) transduction cascade. Radially decreasing glutamate levels around the ribbon release site are effected by diffusion and transporter (black serrated border) losses. Dendrites near the ribbon

expressing mGluR6 (cone ON BC) or AMPA receptors (HC) access perhaps a 30–90x higher glutamate level than peripheral dendrites (OFF BC) expressing more sensitive KA receptors (see Devries et al.[23]). Enhanced KA receptor expression by reprogrammed rod BCs could render them responsive once again. **C** The canonical high-sensitivity scotopic pathway of the mammalian retina. Rods drive rod ON bipolar cells via sign-inverting (−) mGluR6 synapses and cones drive OFF bipolar cells mostly via sign-conserving (+) KA receptors and ON bipolar cells via sign-inverting mGluR6 synapses. Cone bipolar cells alone directly drive ganglion cells with sign-conserving AMPA receptors, creating distinct cone OFF (filled cells) and cone ON (open cells) channels that culminate in ganglion cell spiking to light decrements and increments respectively. In scotopic conditions, cones are silent and rods capture cone bipolar cell channels via an intercalary neuron, a glycinergic rod amacrine cell that receives sign-conserving input directly from rod bipolar cells and distributes those signals to ON cone bipolar cell terminals via sign-conserving gap junctions or OFF cone bipolar cell terminals via sign-inverting glycinergic synapses. Tracing the hyperpolarizing rod response to a flash of light reveals that this network preserves the polarity of ON and OFF channel signaling. **D** In cone-sparing RP, survivor rod bipolar cells attempt to contact cones. If such cells reprogram by expressing iGluRs, a collision network emerges, corrupting cone pathway signaling driven by remnant functional cones.